

ARTICLE OPEN



tiRNA-Val-CAC-2 interacts with FUBP1 to promote pancreatic cancer metastasis by activating *c-MYC* transcription

Qunli Xiong^{1,3}, Yaguang Zhang^{2,3}, Yongfeng Xu¹, Yang Yang¹, Zhiwei Zhang¹, Ying Zhou¹, Su Zhang², Lian Zhou², Xiaowen Wan², Xiaojuan Yang¹, Zhu Zeng¹, Jinlu Liu¹, Ying Zheng¹, Junhong Han²✉ and Qing Zhu¹✉

© The Author(s) 2024

Cumulative studies have established the significance of transfer RNA-derived small RNA (tsRNA) in tumorigenesis and progression. Nevertheless, its function and mechanism in pancreatic cancer metastasis remain largely unclear. Here, we screened and identified tiRNA-Val-CAC-2 as highly expressed in pancreatic cancer metastasis samples by tsRNA sequencing. We also observed elevated levels of tiRNA-Val-CAC-2 in the serum of pancreatic cancer patients who developed metastasis, and patients with high levels of tiRNA-Val-CAC-2 exhibited a worse prognosis. Additionally, knockdown of tiRNA-Val-CAC-2 inhibited the metastasis of pancreatic cancer in vivo and in vitro, while overexpression of tiRNA-Val-CAC-2 promoted the metastasis of pancreatic cancer. Mechanically, we discovered that tiRNA-Val-CAC-2 interacts with FUBP1, leading to enhanced stability of FUBP1 protein and increased FUBP1 enrichment in the *c-MYC* promoter region, thereby boosting the transcription of *c-MYC*. Of note, rescue experiments confirmed that tiRNA-Val-CAC-2 could influence pancreatic cancer metastasis via FUBP1-mediated *c-MYC* transcription. These findings highlight a potential novel mechanism underlying pancreatic cancer metastasis, and suggest that both tiRNA-Val-CAC-2 and FUBP1 could serve as promising prognostic biomarkers and potential therapeutic targets for pancreatic cancer.

Oncogene (2024) 43:1274–1287; <https://doi.org/10.1038/s41388-024-02991-9>

INTRODUCTION

Pancreatic cancer has become a prominent public health problem with high morbidity and mortality. According to the global cancer data statistics in 2020, the morbidity and mortality rate of pancreatic cancer ranked 14th and 7th, respectively [1], and it is estimated to become the second leading cause of cancer death by 2030 [2]. Pancreatic cancer patients commonly exhibit inadequate specific clinical symptoms during the initial stages and are thus often diagnosed at advanced stages, with high propensities for metastasis. In particular, the liver frequently serves as the primary destination for pancreatic cancer metastasis, leading to a median survival period below 12 months, thereby posing critical threats to human health [3]. Therefore, screening and identifying early diagnostic markers or potential therapeutic targets for pancreatic cancer has significant implications for improving the quality of life and prognosis of patients with this disease.

Non-coding RNA (ncRNA) refers to a class of RNA which is unable to encode proteins. Recently, the research on the regulatory function of ncRNA in tumors and its interactive relationship with tumor occurrence and development has become a hot topic in the biomedical field [4–6]. tRNA-derived small RNA (tsRNA) is a small fragment RNA of specific size ranging from 15–40 nt generated by specialized nucleases (such as Dicer and angiogenin) cleaving tRNA loops in specific cells or tissues [7, 8]. Accumulated evidence shows that tsRNAs have extensive biological functions [9, 10], including participation in cell and

tissue stress responses [11], protein translation regulation [10], stem cell biology [12], ribosome biogenesis [13], transposon regulation [14], etc. For example, Mo et al. identified low expression of 5'-tiRNA-Val in breast cancer tissue and found negative correlation between the content of 5'-tiRNA-Val in patient serum and tumor stage as well as lymph node metastasis. Further research revealed that 5'-tiRNA-Val inhibits the FZD3/Wnt/ β -catenin signaling pathway and becomes a new tumor suppressor, which may become a potential diagnostic biomarker for breast cancer [15]. Han et al. discovered significant increase of 33 nt tiRNA-Gly in papillary thyroid cancer based on tRFs and tiRNA sequencing. Mechanistic studies showed that tiRNA-Gly directly binds to the UHM domain of splicing related RNA-binding protein RBM17 [16]. Tao and colleagues found the distribution of tsRNAs in human colorectal cancer tissue and confirmed that 5'tiRNA-His-GTG is upregulated in colorectal cancer tissue. In vivo and in vitro experiments revealed the carcinogenic effect of 5'tiRNA-His-GTG in colorectal cancer and found that targeting 5'tiRNA-His-GTG can induce cancer cell apoptosis [17]. Jin et al. identified pancreatic cancer-related tsRNAs using RNA sequencing, RT-qPCR and in situ hybridization (ISH) in human serum, tissue, cancer cells, and mouse models. Changes in tsRNA profiles in serum and tumor tissue provide new biomarkers for early diagnosis and prognosis of pancreatic cancer and revealed that the ISH score of tRF-Pro-AGG-004 and tRF-Leu-CAG-002 in serum can be used as valuable biomarkers for predicting postoperative survival of patients [18].

¹Division of Abdominal Tumor Multimodality Treatment, Cancer Center, Department of General Surgery, West China Hospital, Sichuan University, Chengdu 610041, China.

²Department of Biotherapy, Cancer Center and State Laboratory of Biotherapy, and Frontiers Science Center for Disease-related Molecular Network, West China Hospital, Sichuan University, Chengdu 610041, China. ³These authors contributed equally: Qunli Xiong, Yaguang Zhang. ✉email: hjunhong@scu.edu.cn; newzhuqing1972@scu.edu.cn

Received: 12 October 2023 Revised: 19 February 2024 Accepted: 20 February 2024

Published online: 5 March 2024

Together, tsRNAs have important biological functions and potential clinical application in tumors.

In this study, we identified 226 tsRNAs which has significantly differential expression in primary and metastatic pancreatic cancer patients, including 120 upregulated- and 106 downregulated-tsRNAs. Notably, tiRNA-Val-CAC-2 was significantly upregulated in metastatic lesions of pancreatic cancer patients. Overexpression of tiRNA-Val-CAC-2 promoted migration and invasion of pancreatic cancer cells, while knockdown of tiRNA-Val-CAC-2 inhibited these processes. Further mechanistic investigations revealed that tiRNA-Val-CAC-2 could interact with RNA-binding protein FUBP1, leading to the increase of FUBP1 protein stability, which further promotes pancreatic cancer metastasis by *c-MYC* transcription. Taken together, our findings uncovered a novel mechanism in which a tsRNA, tiRNA-Val-CAC-2, regulates pancreatic cancer metastasis, indicating that tiRNA-Val-CAC-2 and FUBP1 could serve as promising therapeutic targets for pancreatic cancer.

RESULTS

tsRNAs are differentially expressed between primary and metastatic tissues in pancreatic cancer

To identify and characterize differentially expressed tsRNA, we compared the tsRNA expression profiles between primary tissues and liver metastasis tissues in pancreatic cancer. The clinical information of these samples were showed in Supplementary Table 4. The principal component analysis (PCA) revealed the distinctive expression difference between the primary group and the metastatic group (Fig. 1A). The correlation coefficient analysis indicated a significant correlation between the two groups (Fig. 1B). According to previous research [19], we classified tsRNA into four types, including tsRNA-5, tsRNA-3, tRF-i, tRF-U (Fig. 1C), which account for 57.8%, 32.5%, 9.1%, 0.6% in metastatic group and 65.0%, 29.6%, 4.9%, 0.5% in primary group, respectively (Fig. 1D). Compared with the primary group, more tsRNAs in the range of 14 to 18 nt was detected in the metastatic tumor group. The differential expression of tsRNA between 14 and 16 nt was primarily due to tsRNA-5, while tsRNA-3 accounted for the majority of the differential tsRNA expression between 17 and 18nt (Fig. 1E). We further analyzed the tsRNA produced by different tRNAs. The results revealed that the amount of tsRNA derived from tRNA-Ala-AGC, tRNA-Gln-TTG, tRNA-Lys-TTT, tRNA-Ser-TGA, and tRNA-Val-CAC was higher in the metastatic group than in the primary group. Among the differential tsRNA species, tsRNA-5 was the most prevalent type (Fig. 1F). Subsequent analysis of tsRNA sequencing data revealed the presence of 350 tsRNAs. Of these, 127 and 18 unique tsRNAs were detected in the metastatic and primary groups, respectively (Fig. 1G). The heatmap and scatter plot were utilized to visualize the expression levels and distribution patterns of tsRNAs within the primary and metastatic groups (Fig. 1H, I). As shown in Fig. 1H, a total of 226 differentially expressed tsRNAs in the two groups were identified. Among these, 120 tsRNAs were found to be upregulated, while 106 tsRNAs were down-regulated in metastatic groups. The results clearly demonstrated a significant difference in the expression profiles of tsRNAs between primary and metastatic tissues in pancreatic cancer.

tiRNA-Val-CAC-2 is up-regulated in metastatic pancreatic cancer

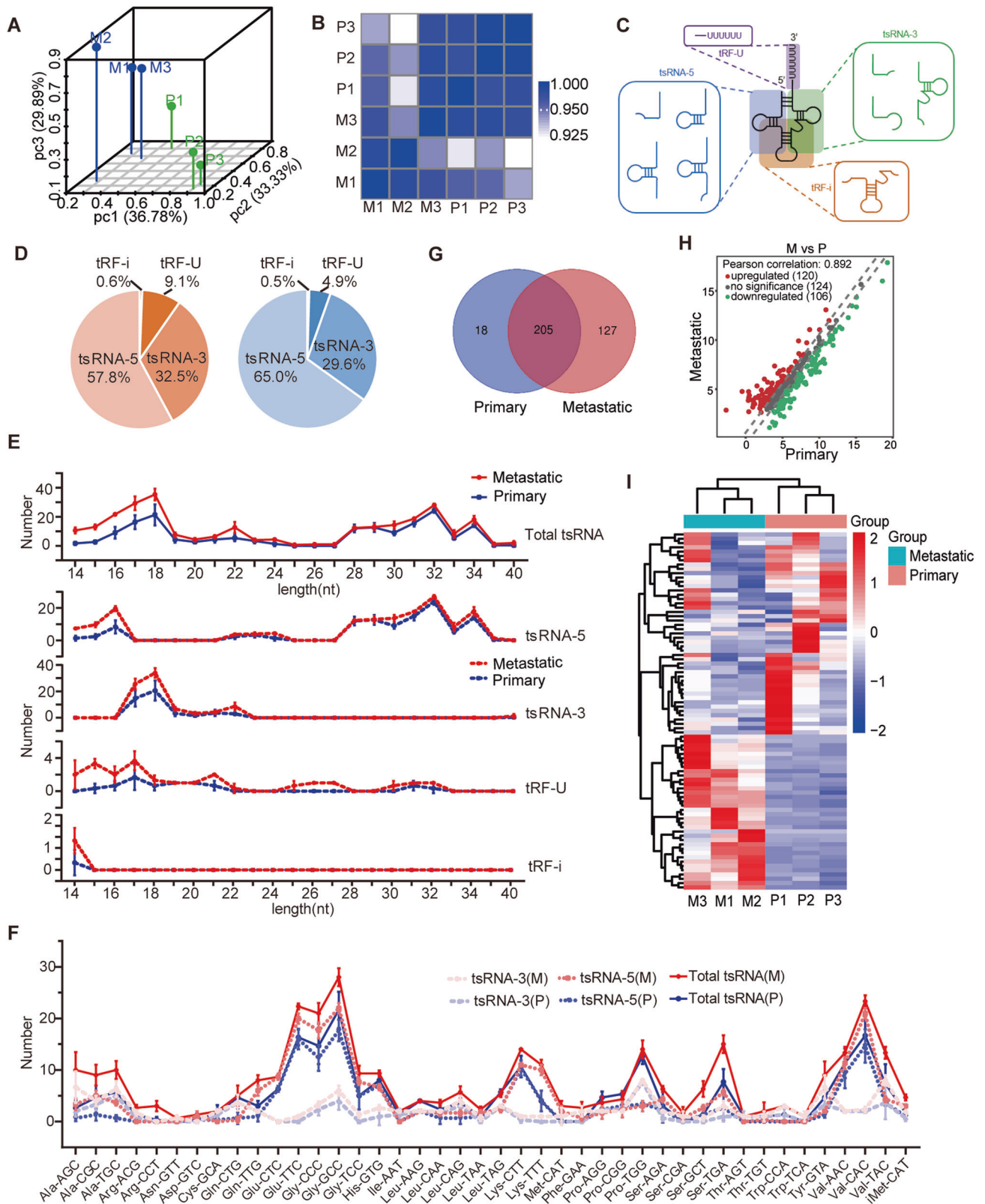
Accumulative evidence has indicated that tiRNAs, whose cleavage site locates on the anticodon of tRNA, are closely related to tumor development [20]. Aberrantly expressed tiRNAs in human solid tumors may be promising diagnostic biomarkers or therapeutic targets [16, 21, 22]. After taking into account the abundance of tiRNAs (measured in counts per million, CPM), statistical significance (p -value < 0.05), and the magnitude of differential expression ($|\log_2FC| > 1.5$), we identified five tiRNAs for further investigation, including tiRNA-Val-CAC-2, tiRNA-Lys-CTT-3, tiRNA-Lys-TTT-3-M2, tiRNA-Lys-CTT-1-M2, and tiRNA-Val-CAC-1-M3

(Supplementary Table 5). Agarose gel electrophoresis was employed to detect the PCR products of the five selected tiRNAs, which displayed a single band of approximately 126 bp in size (Fig. 2A). Subsequently, the products were confirmed by sequencing (Fig. 2B), with the sequences of tiRNA-Val-CAC-2, tiRNA-Lys-CTT-3, tiRNA-Lys-CTT-1-M2, and tiRNA-Val-CAC-1-M3 matching those obtained from tsRNA sequencing. However, the sequence of tiRNA-Lys-TTT-3-M2 did not match that derived from the same samples. Therefore, we proceeded to include the four matched tiRNAs in further RT-qPCR verification. The expression levels of tiRNA-Val-CAC-2 and tiRNA-Lys-CTT-3 were significantly higher in the metastatic samples, as observed from the same RNA samples used for tsRNA sequencing. Conversely, no significant difference was found in the expression levels of tiRNA-Lys-CTT-1-M2 and tiRNA-Val-CAC-1-M3 between the two groups (Fig. 2C). Further analysis using the tRNadb database (<http://trna.bioinf.uni-leipzig.de/DataOutput/Search>) confirmed that tiRNA-Val-CAC-2 and tiRNA-Lys-CTT-3 were 5'-tiRNA fragments derived from tRNA-Val-CAC and tRNA-Lys-CTT, respectively (Fig. 2D). Analysis of the mature tRNA sequences revealed that tiRNA-Val-CAC-2 was 34 nt long (5'-GCTTCTGTAGTGTAGTGGTTATCACGTTTCGCCTC-3'), with the cleavage site located on the anticodon loop (CAC) (Fig. 2D). Similarly, tiRNA-Lys-CTT-3 was 34 nt in length (5'-GCCCGCTAGCTCAGTCGGTAGAGCATGAGACCC-3'), with the cleavage site situated on the anticodon loop (CTT) (Fig. 2D). Independent validation of the two tiRNAs demonstrated that the expression of tiRNA-Val-CAC-2 was significantly higher in the metastatic samples ($n=7$) compared to that in the primary tumors ($n=13$), while no significant difference was observed in the expression levels of tiRNA-Lys-CTT-3 between these two groups (Fig. 2E).

In addition to tissue samples, further validation of tiRNA-Val-CAC-2 was conducted using independent serum samples, consisting of 40 serum samples from pancreatic cancer patients without distant metastasis and 30 serum samples from pancreatic cancer patients with distant metastasis. The results demonstrated that tiRNA-Val-CAC-2 was expressed at significantly higher levels in the serum of patients with metastases than in those without distant metastasis (Fig. 2F). The association between the serum level of tiRNA-Val-CAC-2 and various clinical characteristics (such as age, gender, tumor stage, tumor grade, tumor size, tumor location, smoking, serum CA199, and serum CEA levels) was evaluated using the chi-square test. The analysis revealed a significant correlation between the level of tiRNA-Val-CAC-2 and age and TNM stage, while no significant correlations were observed with gender, tumor grade, tumor size, tumor location, smoking status, serum CA199, and serum CEA levels (Table 1). Prognostic data from patients with pancreatic cancer were gathered, and the serum level of tiRNA-Val-CAC-2 was classified as either high or low using R language software for prognostic analysis. The results indicated that a high level of tiRNA-Val-CAC-2 in the serum was significantly associated with poor prognosis, as shown in Fig. 2G. Moreover, the Cox proportional hazards model was utilized to conduct univariate analysis, highlighting high levels of tiRNA-Val-CAC-2 ($p < 0.001$) and TNM stage ($p = 0.006$) as significant risk factors influencing clinical survival in pancreatic cancer patients (Table 2). In addition, multivariate analysis was conducted, revealing that both the serum level of tiRNA-Val-CAC-2 (HR = 3.195, $p = 0.001$) and TNM stage (HR = 2.258, $p = 0.012$) were informative prognostic markers for clinical outcomes in patients (Table 3). These findings suggest that tiRNA-Val-CAC-2 could serve as a potential prognostic biomarker in patients with pancreatic cancer.

tiRNA-Val-CAC-2 promotes metastasis of pancreatic cancer in vitro and in vivo

To investigate the role of tiRNA-Val-CAC-2 in pancreatic cancer, we first examined its expression and localization in pancreatic cancer



cell lines. RT-qPCR results showed that the expression of tiRNA-Val-CAC-2 in most pancreatic cancer cells was higher than that in normal pancreatic ductal epithelial cells (hTERT-HPNE and HPDE) (Fig. 3A). To investigate the localization of tiRNA-Val-CAC-2 in cells, we employed nucleoplasmic separation assay and found that

tiRNA-Val-CAC-2 was present in both the cytoplasm and nucleus of PANC-1 cells and AsPC-1 cells (Fig. 3B).

Subsequently, we synthesized mimic and inhibitor of tiRNA-Val-CAC-2 in order to investigate its impact on pancreatic cancer cell metastasis. Results of migration and invasion assays showed that

Fig. 1 The overview of the tsRNAs expressions in three primary pancreatic cancer tissues and liver metastases tissues of pancreatic cancer. **A** The principal component analysis (PCA) of tsRNAs expressions in primary and metastatic pancreatic cancer samples. M: metastatic pancreatic cancer. P: primary pancreatic cancer. **B** Correlation heatmap analysis of tsRNAs expressions in primary and metastatic pancreatic cancer samples. M: metastatic pancreatic cancer. P: primary pancreatic cancer. **C** Schematic diagram of tsRNA classification. **D** The distribution of tsRNAs subtype numbers in primary (right panel) and metastatic samples (left panel). **E** Length of different tsRNA classifications and number in primary and metastatic samples. **F** The numbers of subtype tsRNAs against tRNA isodecoders in primary and metastatic pancreatic cancer sample. M: metastatic pancreatic cancer. P: primary pancreatic cancer. **F** The distribution of tsRNAs subtype numbers in primary and metastatic samples. **G** Venn diagram based on number of commonly expressed and specifically expressed tsRNAs in primary and metastatic samples. The scatter plot (**H**) between and heatmap (**I**) of tsRNAs in primary and metastatic pancreatic cancer samples. M: metastatic pancreatic cancer; P: primary pancreatic cancer.

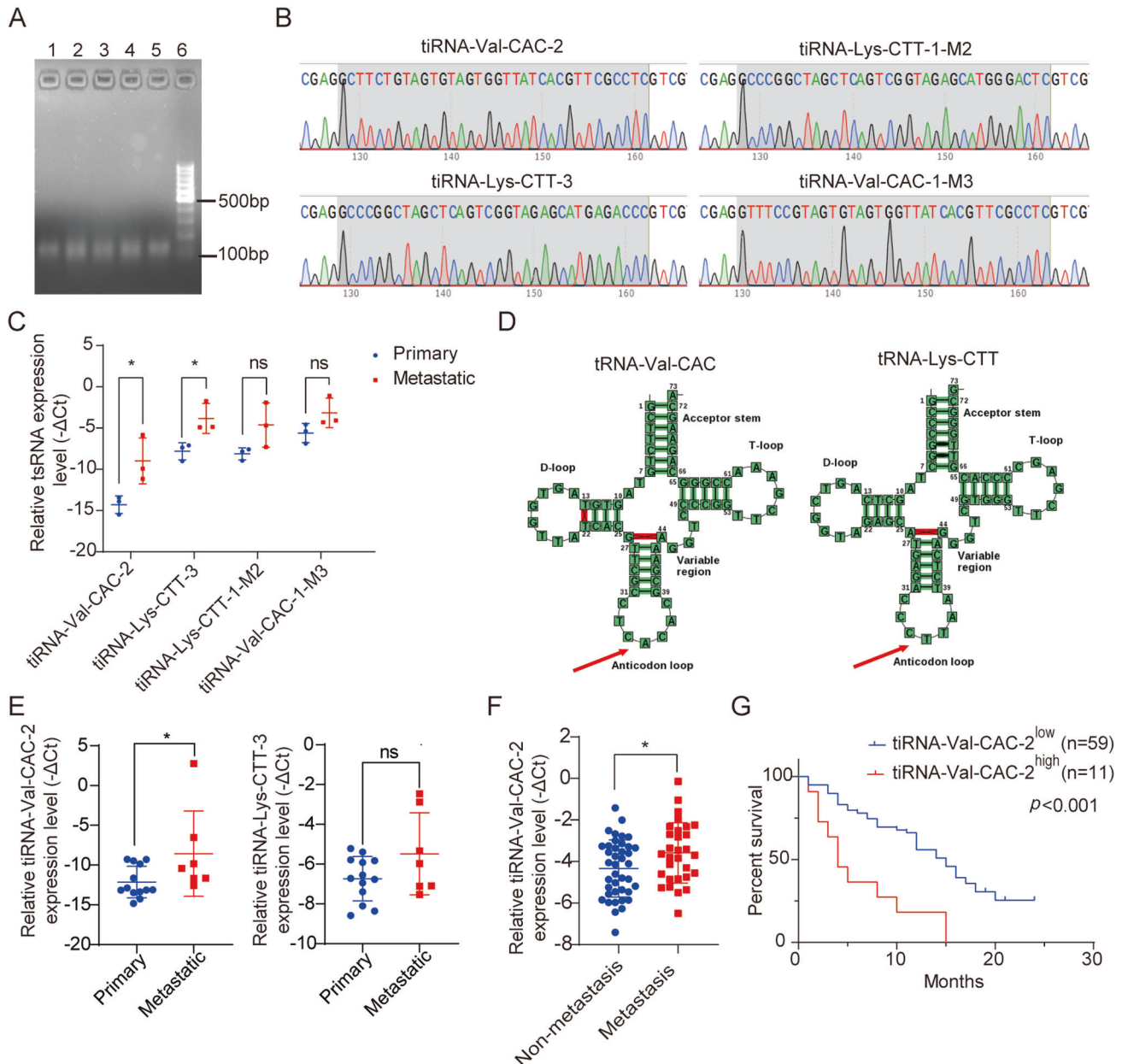


Fig. 2 tiRNA-Val-CAC-2 is highly expressed in pancreatic cancer patients with metastatic and is a potential prognostic biomarker for pancreatic cancer. **A** Agarose gel electrophoresis of PCR products of tsRNAs. Lane 1: tiRNA-Val-CAC-2, Lane 2: tiRNA-Lys-CTT-3, Lane 3: tiRNA-Lys-TTT-3-M2, Lane 4: tiRNA-Lys-CTT-1-M2, Lane 5: tiRNA-Val-CAC-1-M3, Lane 6: Marker. **B** Sanger sequencing results of tsRNAs. **C** RT-qPCR was used to analyze the expression of tiRNA-Val-CAC-2, tiRNA-Lys-CTT-3, tiRNA-Lys-CTT-1-M2, and tiRNA-Val-CAC-1-M3 in three primary and metastatic pancreatic cancer samples which were identical to the tsRNA sequencing samples. **D** Cleavage sites of tiRNA-Val-CAC-2 and tiRNA-Lys-CTT-3 from precursor tRNAs by tRNAdb database. **E** Relative expression of tiRNA-Val-CAC-2 and tiRNA-Lys-CTT-3 in independent primary and metastatic pancreatic cancer tissues. **F** Relative expression of tiRNA-Val-CAC-2 in serum of pancreatic cancer patients with or without metastases. **G** Kaplan–Meier survival analysis of pancreatic cancer patients according to tiRNA-Val-CAC-2 expression in serum of patients. ns, no significance; * $p < 0.05$.

Table 1. Relationship between the level of tiRNA-Val-CAC-2 and clinicopathological parameters of pancreatic cancer patients.

Parameters		n	Low expression	High expression	χ^2	p-value
Number of patients		70	59	11		
Age	≤60	37	28	9	4.393	0.036*
	>60	33	31	2		
Sex	Male	46	39	7	0.025	1.000
	Female	24	20	4		
TNM stage	I–II	20	37	3	4.755	0.045*
	III–IV	50	22	8		
Size	≤3 cm	23	21	2	1.434	0.310
	>3 cm	45	36	9		
	Loss	2				
Location	Head or neck	46	40	6	0.723	0.493
	Body or tail	24	19	5		
Grade	Well and moderate	13	12	1	0.020	1.000
	Poor	22	20	2		
	Loss	35				
Smoke	No	49	39	10	2.516	0.157
	Yes	20	19	1		
	Loss	1				
Preoperative CA19-9 value	<37	13	10	3	0.564	0.428
	≥37	55	47	8		
	Loss	2				
Preoperative CEA value	<5	42	35	7	0.019	1.000
	≥5	26	22	4		
	Loss	2				

* $p < 0.05$ was considered statistically significant.

Table 2. Univariate Cox proportional hazards analysis for survival of pancreatic cancer patients.

Variable	Hazard ratio	95% confidence interval	p-value
tiRNA-Val-CAC-2 expression (high/low)	3.513	1.749–7.055	<0.001*
Age (>60/≤60)	0.814	0.472–1.401	0.458
Gender (male/female)	0.843	0.484–1.466	0.545
TNM stage (III–IV/I–II)	2.407	1.280–4.527	0.006*
Grade (poor/moderate and well)	1.628	0.695–3.812	0.262
Size (>3 cm/<3 cm)	1.617	0.887–2.950	0.117
Location (body and tail/head and neck)	1.552	0.892–2.702	0.120
Smoke (yes/no)	0.651	0.353–1.202	0.170
Preoperative CA19-9 value (≥37/<37)	0.587	0.307–1.124	0.108
Preoperative CEA value (≥5/<5)	1.305	0.749–2.273	0.347

* $p < 0.05$ was considered statistically significant.

Table 3. Multivariate Cox proportional hazards analysis for survival of pancreatic cancer patients.

Variables	Hazard ratio	95.0% CI	p-value
TNM stage	2.258	1.194–4.272	0.012*
tiRNA-Val-CAC-2 expression	3.195	1.528–6.454	0.001*

* $p < 0.05$ was considered statistically significant.

overexpression of tiRNA-Val-CAC-2 significantly augmented the migration and invasion capabilities of pancreatic cancer cells. Conversely, knockdown of tiRNA-Val-CAC-2 led to a reduction in the migration and invasion abilities of pancreatic cancer cells (Fig. 3C–G).

Furthermore, we explored the effect of tiRNA-Val-CAC-2 on pancreatic cancer cell metastasis in vivo utilizing a mouse lung metastasis model. Specifically, antagomir NC and antagomir tiRNA-Val-CAC-2 were transfected into CFPAC-1 cells, respectively, and then intravenously injected into nude mice. The progression of lung metastasis was subsequently monitored by utilizing an in vivo imaging system. In vivo bioluminescence

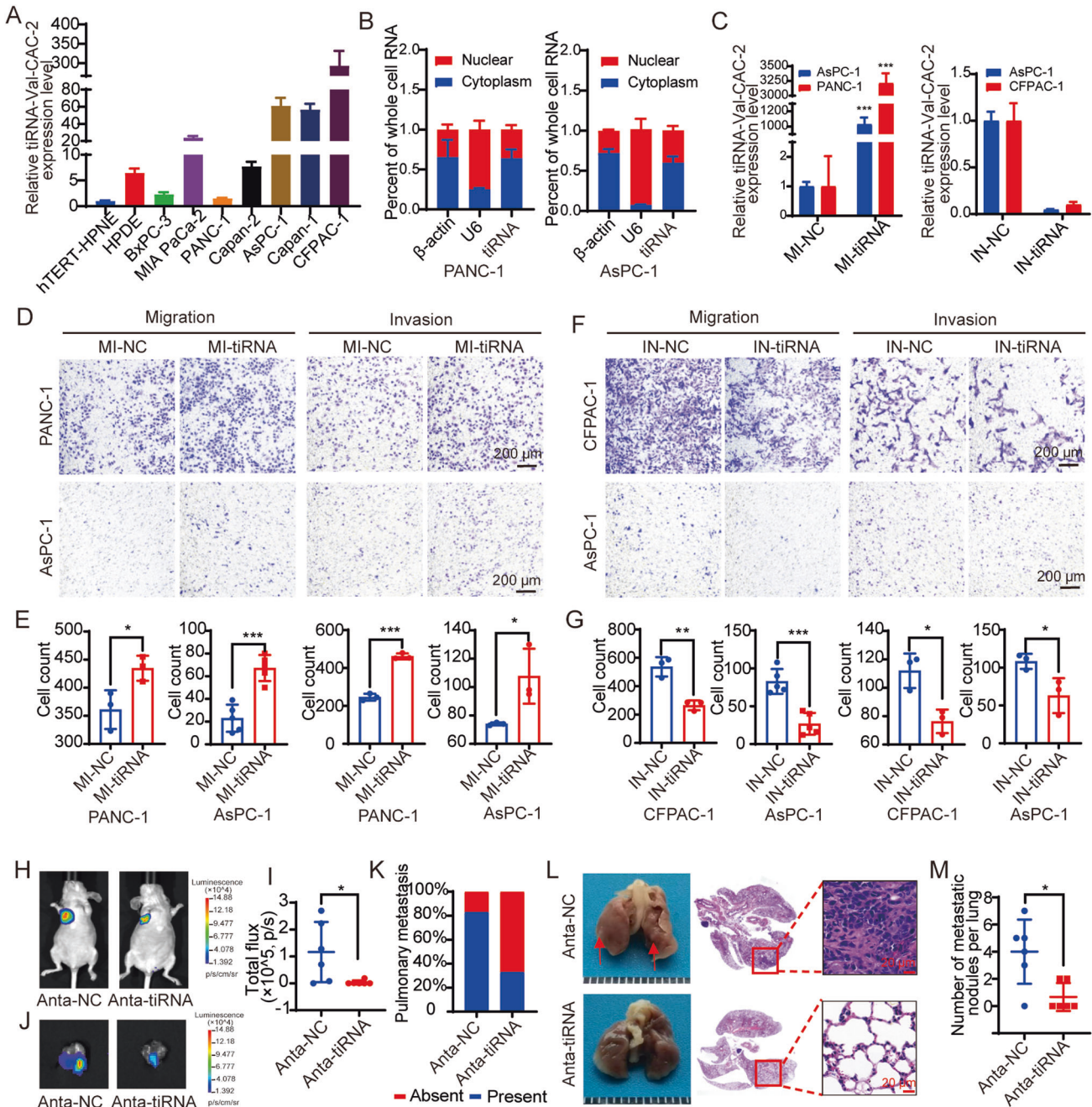


Fig. 3 tiRNA-Val-CAC-2 promotes pancreatic cancer metastasis *in vitro* and *in vivo*. **A** Relative expression levels of tiRNA-Val-CAC-2 in pancreatic cancer cell lines by RT-qPCR. **B** Localization of tiRNA-Val-CAC-2 in pancreatic cancer cells was determined by a nuclear plasma separation assay. β -actin was used as a cytoplasmic marker and U6 was used as a nuclear marker. Effects of knockdown and overexpression of tiRNA-Val-CAC-2 (**C**) on migration and invasion of PANC-1 (**D**), AsPC-1 (**D**, **F**) and CFPAC-1 (**F**) cells, and responding statistical analysis (**E**, **G**). **H**, **I** Nude mice were transplanted with indicated Luc-labeled CFPAC-1 cells *via* tail vein injection, luciferase activity was visualized 4 weeks post-transplantation ($n = 6$). Lung imaging (**J**) and the proportion of lung with metastases in total six lungs (**K**). **L** Light field map of lung tumor nodules (left panel) and HE staining of lung tissue (right panel). **M** Statistics on the number of tumor nodules per lung. MI-NC: mimic NC; MI-tiRNA: mimic tiRNA-Val-CAC-2; IN-NC: inhibitor NC; IN-tiRNA: inhibitor tiRNA-Val-CAC-2; Anta-NC antagonist NC, Anta-tiRNA antagonist tiRNA-Val-CAC-2. * $p < 0.05$, ** $p < 0.01$, *** $p < 0.001$.

imaging demonstrated that both the fluorescence intensity in the lungs and the number of metastatic lungs were significantly lower in the antagonist tiRNA-Val-CAC-2 group than in the control group (Fig. 3H–K). Moreover, tiRNA-Val-CAC-2 knockdown significantly decreased the number of metastatic nodules in the lungs (Fig. 3L, M). These results suggest that tiRNA-Val-CAC-2 plays a key role in the promotion of pancreatic cancer metastasis *in vivo*.

tiRNA-Val-CAC-2 interacts with FUBP1

To further explore the underlying mechanism by which tsRNA regulates the metastasis, we utilized RNA pull-down and mass spectrometry assays to identify tiRNA-Val-CAC-2 associated proteins. We performed RNA pull-down assay using biotin-labeled tiRNA-Val-CAC-2 and the resulted proteins were detected by silver staining. As shown in Fig. 4A, there was a distinct band in the 70–100 kDa position in the sense strand of both cell lines.

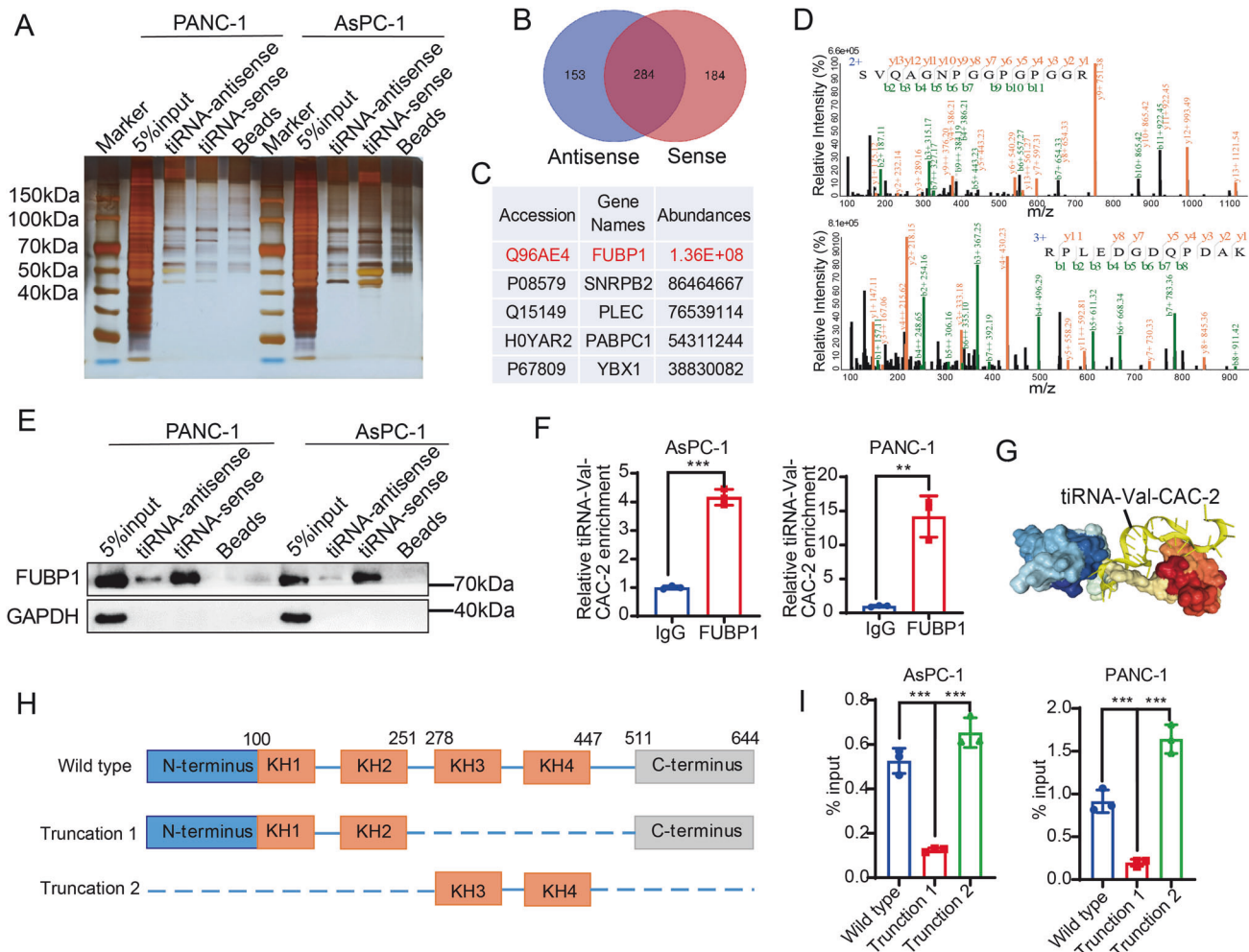


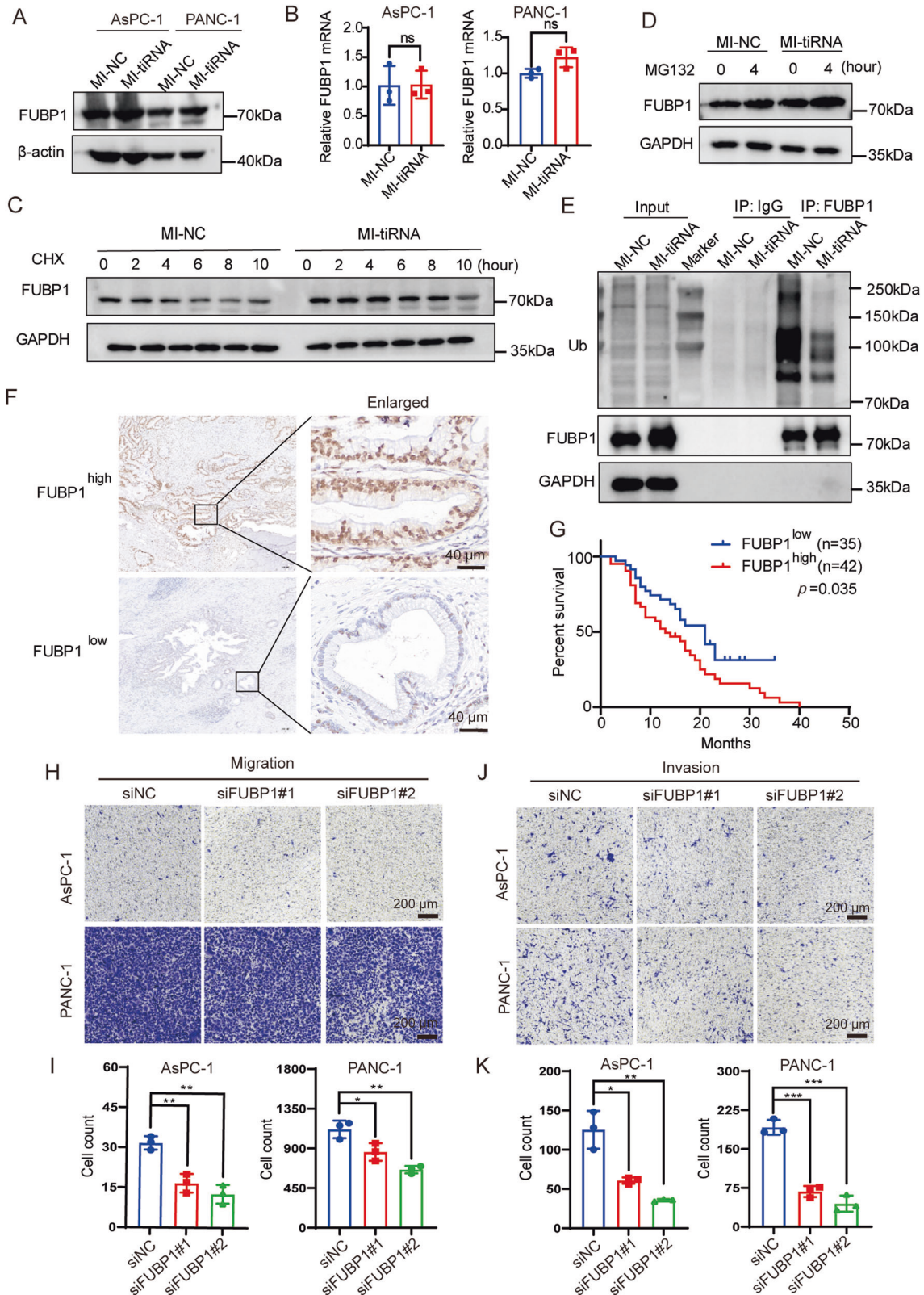
Fig. 4 tiRNA-Val-CAC-2 interacts with RNA-binding protein FUBP1. **A** Silver staining showing affinity capture of proteins from PANC-1 and AsPC-1 cells by RNA pull down. **B** Venn diagram of mass spectrometry results of PANC-1 cells from (A). **C** Top 5 abundant proteins in the sense strand group from mass spectrum. **D** Representative peptide of FUBP1 protein from mass spectrum. **E** FUBP1 protein enrichment in RNA pull down samples by western blot. **F** RIP and RT-qPCR assay were used to test the enrichment of FUBP1 on tiRNA-Val-CAC-2 in AsPC-1 and PANC-1 cells. IgG was used as a negative control. **G** The binding pattern of tiRNA-Val-CAC-2 and FUBP1 protein predicted by HDOCK database. tiRNA-Val-CAC-2 is shown in yellow, which is predicted to bind to the KH3-KH4 domain of FUBP1. **H** Diagram of the full-length and truncated structures of FUBP1. **I** Enrichment of full-length and truncated FUBP1 in tiRNA-Val-CAC-2 was determined by q-PCR after RIP assay. tiRNA-sense: tiRNA-Val-CAC-2; tiRNA-antisense: reverse complementary sequence of tiRNA-Val-CAC-2. * $p < 0.05$, ** $p < 0.01$, *** $p < 0.001$.

Meanwhile, we identified 184 unique proteins in the sense strand group of RNA pull-down samples by mass spectrometry analysis (Fig. 4B). Among these proteins, FUBP1 was identified as the most significant protein, based on the ranking of protein abundance (Fig. 4C). Additionally, two unique major peptides of FUBP1 were detected, as depicted in Fig. 4D. To further validate the mass spectrometry results, we conducted western blot and observed that tiRNA-Val-CAC-2 sense strand was indeed able to pull down more FUBP1 protein compared to the antisense strand (Fig. 4E). Further, we also confirmed the binding between FUBP1 and tiRNA-Val-CAC-2 by RNA immunoprecipitation assay. As shown in Fig. 4F, the results demonstrated that FUBP1 could substantially enrich tiRNA-Val-CAC-2, indicating the interaction between FUBP1 and tiRNA-Val-CAC-2. To gain insight of the binding pattern between tiRNA-Val-CAC-2 to FUBP1, we employed the online database HDOCK (Fig. 4G), and the detailed binding sites of tiRNA-Val-CAC-2 to FUBP1 amino acids were also predicted and shown in supplementary Table 6. These results suggested that tiRNA-Val-CAC-2 mainly binds to the KH3-KH4 domain of FUBP1. In order to validate this prediction, we constructed a wild-type FUBP1 overexpression plasmid, as well as truncated plasmids of FUBP1

lacking the KH3-KH4 domain or only including KH3-KH4 domain as shown in Fig. 4H. RIP experiments were then performed in wild-type and/or mutant FUBP1 transfected AsPC-1 and PANC-1 cells using FLAG antibodies. Results clearly showed that deletion of the KH3-KH4 domain significantly reduced the binding of tiRNA-Val-CAC-2 to FUBP1 (Fig. 4I), indicating that tiRNA-Val-CAC-2 mainly interacts with KH3-KH4 domain of FUBP1 protein.

tiRNA-Val-CAC-2 increases FUBP1 protein stability

To further explore the impact of tiRNA-Val-CAC-2 on FUBP1, we overexpressed tiRNA-Val-CAC-2 in PANC-1 and AsPC-1 cells, and detected FUBP1 expression (Fig. 5A). Interestingly, despite observing an increase of FUBP1 protein upon overexpression of tiRNA-Val-CAC-2, there was no obvious change in its mRNA level (Fig. 5B). And the loss-of-function experiments also indicated that tiRNA-Val-CAC-2 knockdown decreased the FUBP1 protein other than its mRNA (Supplementary Fig. 1A–B). These results prompted us to speculate that tiRNA-Val-CAC-2 may exert its effect on FUBP1 by influencing its protein stability, rather than affecting transcription. To test this possibility, we treated tiRNA-Val-CAC-2 overexpressing or knockdown cell (AsPC-1) with protein synthesis



inhibitor cycloheximide (CHX) and 26S proteasome inhibitor MG132 and collected cell lysates for western blot. As illustrated in Fig. 5C, the treatment with CHX led to a remarkable extension in the half-life of FUBP1 protein in the tiRNA-Val-CAC-2 overexpression group compared to the control group, while

tiRNA-Val-CAC-2 knockdown reduced the FUBP1 protein half-life (Supplementary Fig. 1C). In addition, the inhibition of 26S proteasome with MG132 resulted in a noticeable increase of FUBP1 protein in the tiRNA-Val-CAC-2 overexpression group, as compared to the control group (Fig. 5D), while tiRNA-Val-CAC-2

Fig. 5 **tiRNA-Val-CAC-2 promotes the stability of FUBP1 protein which can be used as a prognostic biomarker.** **A** The protein level of FUBP1 was detected by western blot after overexpression of tiRNA-Val-CAC-2 in AsPC-1 and PANC-1 cells. **B** The mRNA level of FUBP1 was detected by RT-qPCR after overexpression of tiRNA-Val-CAC-2 in AsPC-1 and PANC-1 cells. **C** After the AsPC-1 cells were treated with 100 μ g/mL Cycloheximide (CHX), the half-life of FUBP1 protein was detected by western blot. **D** After AsPC-1 cells were treated with 10 μ M MG132, the effect of tiRNA-Val-CAC-2 on the degradation of FUBP1 protein was detected by western blot. **E** The ubiquitination level of FUBP1 protein was detected by western blot after overexpression of tiRNA-Val-CAC-2 in AsPC-1 cell. **F** Representative immunohistochemical images of FUBP1 high and low expression in pancreatic cancer tissues ($n = 77$). **G** Kaplan–Meier survival analysis of pancreatic cancer patients according to FUBP1 expression. (H–K) Knockdown of FUBP1 inhibited the migration (H, I) and invasion (J, K) of pancreatic cancer cells. mimic NC; MI-tiRNA: mimic tiRNA-Val-CAC-2. * $p < 0.05$, ** $p < 0.01$, *** $p < 0.001$.

Table 4. Relationship between FUBP1 expression and clinicopathological parameters of pancreatic cancer patients.

Parameters		n	Low expression	High expression	χ^2	p-value
Number of patients		77	35	42		
Age	≤60	36	17	19	0.085	0.770
	>60	41	18	23		
Sex	Male	43	20	23	0.044	0.834
	Female	34	15	19		
TNM stage	I–II	74	34	40	0.185	1.000
	III–IV	3	1	2		
Lymph node metastasis	No	53	25	28	0.202	0.653
	Yes	24	10	14		
Grade	Well and moderate	26	17	9	6.289	0.012*
	Poor	51	18	33		
Nerve invasion	Yes	60	28	32	0.161	0.688
	No	17	7	10		
Preoperative CA19-9 value	<37	21	8	13	0.631	0.427
	≥37	56	27	29		
Preoperative CEA value	<5	55	23	32	1.027	0.311
	≥5	22	12	10		

* $p < 0.05$ was considered statistically significant.

knockdown decreased FUBP1 protein expression (Supplementary Fig. 1D). We further examined the effect of tiRNA-Val-CAC-2 on FUBP1 protein ubiquitination. Co-IP assay in AsPC-1 cell showed that overexpression of tiRNA-Val-CAC-2 reduced the ubiquitination level of FUBP1 (Fig. 5E). These results imply that tiRNA-Val-CAC-2 could regulate the stability of FUBP1 protein by decreasing the degradation *via* ubiquitination.

FUBP1 is a potential prognostic biomarker of pancreatic cancer

To explore the role of FUBP1 in pancreatic cancer, immunohistochemical staining was performed on 77 cases of pancreatic cancer. The staining results were divided into high and low expression groups (Fig. 5F). Based on the staining results, we categorized the samples into groups with either high or low expression levels (Fig. 5F). Clinical features and survival data of these patients were also collected and analyzed for potential correlations. The results presented in Table 4 indicated a significant relationship between FUBP1 expression and the tumor grade of pancreatic cancer patients. Specifically, samples from patients with poorly differentiated tumors demonstrated higher FUBP1 expression. However, FUBP1 expression did not exhibit any correlation with patient gender, age, TNM stage, presence of neural invasion, or serum CA199 and CEA expression levels. It is noteworthy that patients with high FUBP1 expression displayed a poorer prognosis compared to those with low FUBP1 expression (Fig. 5G). In addition, univariate analysis with the Cox proportional hazards model identified both high FUBP1 level (HR = 1.771, $p = 0.044$) and tumor grade (HR = 2.090, $p = 0.013$) as statistically significant

risk factors influencing the clinical survival of pancreatic cancer patients (Table 5). These results indicate that FUBP1 can serve as a potential prognostic biomarker for individuals diagnosed with pancreatic cancer. To investigate the impact of FUBP1 on pancreatic cancer cell metastasis, we utilized transwell migration and invasion assays in FUBP1 knockdown pancreatic cancer cells and observed that the obvious reduction in migration and invasion (Fig. 5H–K), indicating that FUBP1 indeed regulates the metastasis of pancreatic cancer.

tiRNA-Val-CAC-2 promotes metastasis of pancreatic cancer by up-regulating *c-MYC* transcription through FUBP1

Previous studies have reported that FUBP1 protein can regulate *c-MYC* transcription by binding to the *c-MYC* far-upstream element (FUSE) sequence, thereby affecting tumor metastasis in lung cancer and breast cancer [23, 24]. To evaluate the potential impact of FUBP1 on *c-MYC* transcription in pancreatic cancer cells, we performed ChIP assays using specific antibody against FUBP1. Results showed that FUBP1 was not substantially enriched in the *c-MYC* promoter region located near the transcription start site (Site 1, Fig. 6A). However, FUBP1 was significantly enriched in the FUSE region (Site 2 and Site 3, Fig. 6A). We further observed a reduction in *c-MYC* expression levels in FUBP1-knockdown pancreatic cancer cells (Fig. 6B, C). Taken together, these results suggest that FUBP1 may play a critical role in the regulation on *c-MYC* transcription in pancreatic cancer probably through interaction with FUSE motif.

Based on the aforementioned findings, we speculated that tiRNA-Val-CAC-2 may be involved in FUBP1-mediated *c-MYC*

Table 5. Univariate Cox proportional hazards analysis for survival of pancreatic cancer patients.

Variable	Hazard ratio	95% confidence interval	p-value
FUBP1 expression (high/low)	1.771	1.017–3.068	0.044*
Age (≤60/>60)	1.359	0.792–2.331	0.265
Gender (female/male)	0.853	0.501–1.452	0.558
TNM stage (III–IV/I–II)	0.210	0.028–1.565	0.128
Grade (poor/moderate and well)	2.090	1.169–3.736	0.013*
Nerve invasion (no /yes)	1.495	0.786–2.845	0.221
Preoperative CA19-9 value (≥37/<37)	1.552	0.845–2.852	0.157
Preoperative CEA value (≥5/<5)	0.670	0.365–1.232	0.198

* $p < 0.05$ was considered statistically significant.

transcription. To test this hypothesis, we firstly measured *c-MYC* mRNA levels by RT-qPCR and found that overexpression of *tiRNA-Val-CAC-2* is able to increase *c-MYC* transcription (Fig. 6D). Next, we performed ChIP assay in cells overexpressing *tiRNA-Val-CAC-2* and found that *tiRNA-Val-CAC-2* promotes the transcription of *c-MYC* by binding to the *c-MYC* FUSE region through FUBP1 (Site 2 and Site 3, Fig. 6E). Since *tiRNA-Val-CAC-2* is capable of promoting FUBP1-mediated *c-MYC* transcription in pancreatic cancer cells, we further hypothesized that *tiRNA-Val-CAC-2* may promote metastasis in pancreatic cancer through FUBP1 to active *c-MYC* transcription. To verify this possibility, we conducted rescue experiments in AsPC-1 and PANC-1 cells and observed an increase in both the protein levels of *c-MYC* and FUBP1 following the overexpression of *tiRNA-Val-CAC-2* (Fig. 6F). Of note, we found that both protein level and mRNA level of *c-MYC* in the rescue group were successfully restored by FUBP1 knockdown when compared to overexpression *tiRNA-Val-CAC-2* group (Fig. 6F–H). Additionally, we also found that overexpression of FUBP1 successfully reversed *c-MYC* protein and mRNA levels in the rescue group as compared with the *tiRNA-Val-CAC-2* knockdown group (Supplementary Fig. 2A, B). Furthermore, the results from transwell migration and invasion assays revealed that FUBP1 knockdown attenuate the ability of *tiRNA-Val-CAC-2* in promoting cancer cell migration and invasion (Fig. 6I–L). As we expected, FUBP1 can improve the reduced ability of migration and invasion caused by *tiRNA-Val-CAC-2* knockdown (Supplementary Fig. 2C, D). These findings provide further evidence in support of notion that *tiRNA-Val-CAC-2* promotes the metastasis through the FUBP1-mediated activation of *c-MYC* transcription in pancreatic cancer (Fig. 6M).

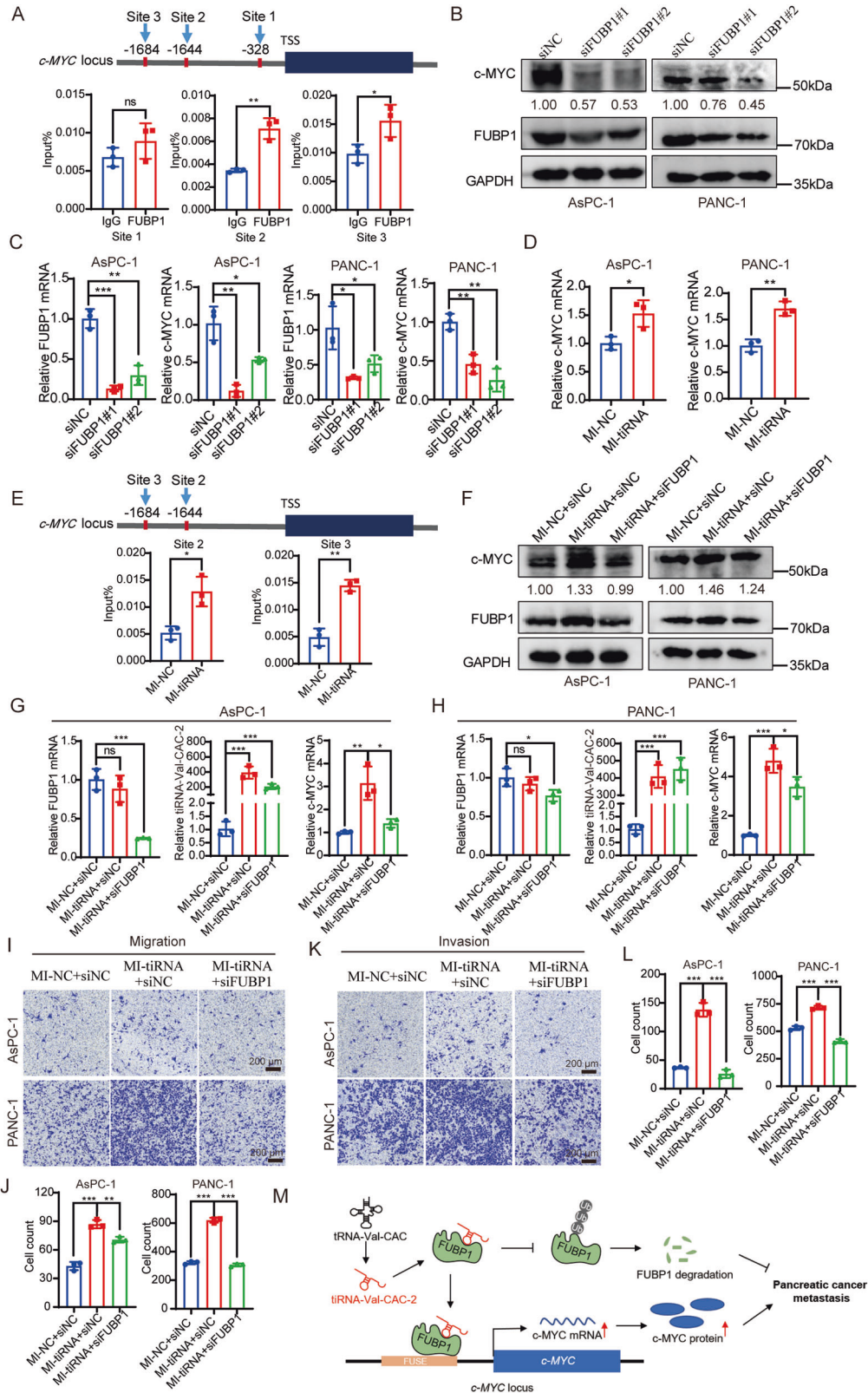
To investigate the potential influence of *tiRNA-Val-CAC-2* on pancreatic cancer metastasis through FUBP1 in vivo, we conducted rescue animal experiments. The result revealed that *tiRNA-Val-CAC-2* overexpression significantly promoted lung metastasis of PANC-1 cells in vivo. However, when FUBP1 was knocked down, the metastatic effect induced by *tiRNA-Val-CAC-2* was counter-balanced (Fig. 7A–F). Furthermore, we investigated the association between *tiRNA*, FUBP1, and *c-MYC* using tumor samples obtained from 12 pancreatic cancer patients. Remarkably, we observed a consistent expression pattern of these three factors in most of the tumor patients (Fig. 7G–I). Moreover, a statistically significant correlation was found among them (Fig. 7J). Taken together, our findings unearthed differences in *tsRNA* expression between primary and metastatic pancreatic cancer, as well as highlighted the high abundance of a novel *tiRNA*, referred to as *tiRNA-Val-CAC-2*. Knockdown of *tiRNA-Val-CAC-2* restricted the metastatic potential of pancreatic cancer cells. Mechanistically, *tiRNA-Val-CAC-2* interacts with the KH3-KH4 domain of FUBP1 to inhibit FUBP1 degradation. Thus, in turn, it leads to the accumulation of FUBP1 protein at the far-upstream element (FUSE) of the *c-MYC* proto-oncogene, which facilitates *c-MYC* transcription and

ultimately results in the metastasis (Fig. 6M). Importantly, we also discovered that *tiRNA-Val-CAC-2* is highly expressed in the serum of pancreatic cancer patients with metastasis, high levels of *tiRNA-Val-CAC-2* are closely related with poor prognosis. These findings shed light on the potential of *tiRNA-Val-CAC-2* serving as a prognostic biomarker and therapeutic target for pancreatic cancer.

DISCUSSION

tsRNAs were originally believed to be random degradation products of *tRNAs*. However, it is now widely recognized that the expression of certain *tsRNAs* is formed by specific selective cleavage of *tRNAs* under certain stress, which relies on specific enzymes such as angiogenin (ANG), RNase T2, and RNase L [25, 26]. Therefore, it is necessary to distinguish between small RNAs generated solely from the degradation of longer transcripts and functional small RNAs. In this study, we observed a significant presence of *tsRNAs* in the size range of 16–18 nt and 31–33 nt through *tsRNA* sequencing. This observation aligns with previous research conducted by Cole et al. [27], which reported similar length patterns for *tsRNA-5* (32–33 nt) and *tsRNA-3* (16–18 nt). Additionally, we noticed a distinct peak of *tsRNA-5* in the 14–16 nt range. Due to the construction and sequencing of small RNA libraries often generating fragments from various non-coding RNAs such as ribosomal RNA, transfer RNA, small nucleolar RNA, and small nuclear RNAs [27], it cannot be ruled out that the presence of *tsRNA-5* in the 14–16 nt might be attributed to *tRNA* degradation processes.

Cancer remains the leading cause of mortality globally, with poor prognoses for many patients due to the absence of reliable early diagnostic markers and effective anti-cancer treatments. However, the emergence of *tsRNAs* as a novel class of small non-coding RNAs has opened up new perspectives for the development of diagnostic biomarkers and therapeutic targets for cancer. For example, Wu et al. found that the combination of plasma 5'-TRF-Gly-GCC with carcinoembryonic antigen and carbohydrate antigen 199 in colon cancer patients increased the AUC value to 0.926 [28]; Importantly, Panoutsopoulou et al. found a significant correlation between i-TRF-GlyGCC and early progression as well as poor overall survival [29]; In addition, Li et al. discovered that the expression level of serum tRF-29-R9J8909NF5JP is significantly elevated in gastric cancer tissues, and its high expression is associated with lower survival rates [30]. In this study, we found that the expression of *tiRNA-Val-CAC-2* is significantly upregulated in metastatic lesions of pancreatic cancer compared to primary lesions, and patients with high expression of serum *tiRNA-Val-CAC-2* demonstrated a poorer prognosis. Furthermore, we found that *tiRNA-Val-CAC-2* plays a critical role in promoting metastasis in pancreatic cancer. Of note, Mo et al. reported that 5'-*tiRNA-Val* acts as a potential tumor-suppressor via FZD3-mediated Wnt/



beta-catenin signaling pathway in the progression of breast cancer [15]. Regarding the different roles of the two tsRNAs derived from the same mature tRNA in tumor, there are some potential explanations. Firstly, the sequence and size of the two tsRNAs are not exactly the same. Secondly, the mechanism of

action of 5'-tiRNA-Val discovered by Mo et al. is completely different from that of tiRNA-Val-CAC-2 found by our study. Alternatively, it may be caused by different tumor types. Many studies have found that the same gene may play different functions in different tumors, and some even are completely

Fig. 6 **tiRNA-Val-CAC-2 facilitates pancreatic cancer metastasis by up-regulating c-MYC transcription through interaction with FUBP1.** **A** Chromatin immunoprecipitation (ChIP) analysis of FUBP1 enrichment on upstream of *c-MYC* transcription start site in AsPC-1 cells. FUBP1 knockdown inhibited the expression of *c-MYC* protein (**B**) and mRNA (**C**) in AsPC-1 and PANC-1 cells by western blot and RT-qPCR assay. **D** tiRNA-Val-CAC-2 overexpression increased the expression of *c-MYC* mRNA in AsPC-1 and PANC-1 cells by RT-qPCR assay. **E** ChIP analysis of FUBP1 enrichment on FUSE element of *c-MYC* in AsPC-1 cells after tiRNA-Val-CAC-2 overexpression. The protein (**F**) and mRNA (**G**, **H**) expression of *c-MYC* was measured in control, tiRNA-Val-CAC-2 overexpression, and rescue groups by western blot and RT-qPCR. The migration (**I**, **J**) and invasion (**K**, **L**) abilities were measured in control, tiRNA-Val-CAC-2 overexpression, and rescue groups by transwell assay. **M** Schematic diagram of tiRNA-Val-CAC-2 promoting metastasis in pancreatic cancer. By interacting with FUBP1, tiRNA-Val-CAC-2 maintained the stability of FUBP1, increased FUBP1 enrichment in the FUSE region of *c-MYC* gene, promoted the transcription of proto-oncogene *c-MYC*, and eventually led to pancreatic cancer metastasis. FUSE: far-upstream element sequence. MI-NC: mimic NC; MI-tiRNA: mimic tiRNA-Val-CAC-2. ns no significance; * $p < 0.05$, ** $p < 0.01$, *** $p < 0.001$.

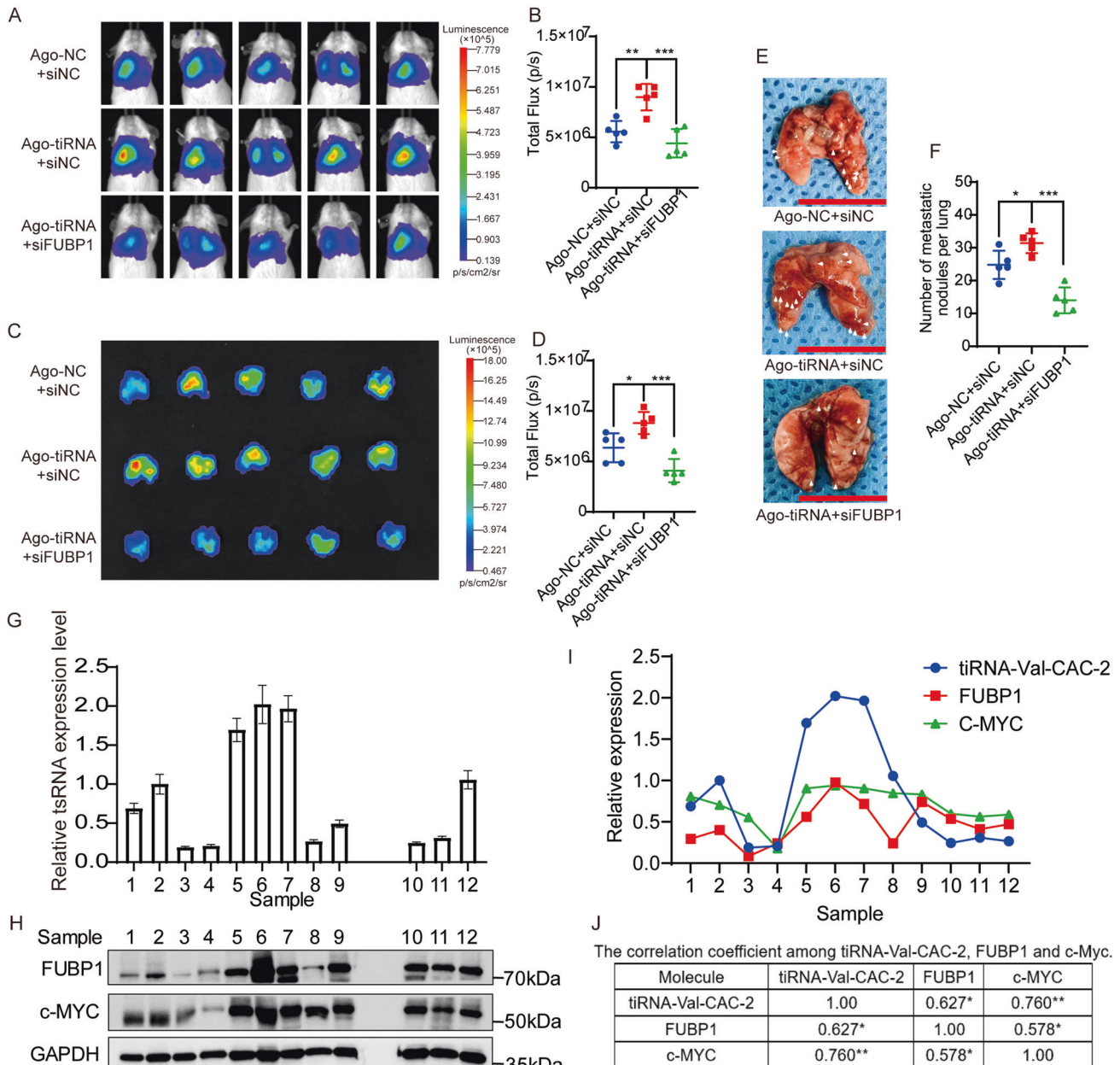


Fig. 7 **tiRNA-Val-CAC-2 facilitates pancreatic cancer metastasis by FUBP1 in vivo, and the correlation among tiRNA-Val-CAC-2, FUBP1 and c-MYC.** **A**, **B** Mice were transplanted with indicated Luc-labeled PANC-1 cells *via* tail vein injection, luciferase activity was visualized 20-days post-transplantation ($n = 5$). **C**, **D** Lung imaging and total fluorescence statistics. **E**, **F** Light field of lung tumor nodules and statistics on the number of tumor nodules per lung. Scar bar=1 cm. **G** The expression of tiRNA-Val-CAC-2 in tumor tissues from 12 patients with pancreatic cancer via RT-qPCR. **H** Western blot was used to detect the protein expression of FUBP1 and c-MYC in tumor tissues from 12 patients with pancreatic cancer. **I** The expression of tiRNA-Val-CAC-2, FUBP1 and c-MYC in tumor tissues from 12 patients with pancreatic cancer by quantitative analysis. **J** The correlation coefficient among tiRNA-Val-CAC-2, FUBP1 and c-Myc. Ago-NC: agomir NC; Ago-tiRNA: agomir tiRNA-Val-CAC-2; * $p < 0.05$, ** $p < 0.01$, *** $p < 0.001$.

opposite. For example, ID4 gene is typically highly expressed in normal prostate tissue but exhibits decreased expression in prostate cancer tissue and gradually decreases with cancer progression, highlighting the conventional inactivation pattern of a tumor-suppressor gene. However, the ID4 gene may act as a proto-oncogene, either being highly expressed in tumor tissue or exhibiting an increased copy number in bladder cancer [31]. Of course, other more plausible explanations are need to be further explored.

In addition, recent studies have shown that tsRNAs can be present in extracellular vesicles, such as exosomes, in the blood. For example, Zhu et al. observed the widespread presence of tsRNAs in exosomes and identified four tsRNAs that are significantly elevated in the plasma of liver cancer patients [32]. However, our study examined the total tsRNA in the serum, and whether tsRNAs exist in the form of extracellular vesicles, specifically exosomes, in the serum requires further exploration.

Different tsRNAs have distinct functions and mechanisms of action. Chen et al. summarized three primary mechanisms of tsRNAs from an evolutionary perspective, including tRNA mimicry/displacement, formation of tsRNA-ribonucleoproteins complexes, and association with Argonaute proteins [33]. Yu et al. concluded that tsRNAs play important roles in RNA silencing, translation regulation, and epigenetic modulation [34]. For example, tRF-Val directly binds to EEF1A1, facilitating the transport of EEF1A1 to the nucleus and enhances its interaction with MDM2, ultimately resulting in the inhibition of the downstream molecular pathways of P53 and promoting gastric cancer progression [35]. AS-TDR-007333 activates *MED29* to further promote malignant transformation of non-small cell lung cancer cells through two different mechanisms. AS-TDR-007333 interacts with HSPB1 to enhance the H3K4me1 and H3K27ac in *MED29* promoter to activate *MED29* expression. Additionally, AS-TDR-007333 triggers an increase in the expression of transcription factor ELK4, which binds to the *MED29* promoter and further promotes its transcriptional activity [36]. Using RNA pull down and mass spectrometry analysis, we identified that tiRNA-Val-CAC-2 can interact with RNA-binding protein FUBP1. FUBP1 is a type of fusion binding protein that has the ability to recognize single-stranded DNA, and it belongs to the FUBP protein family [37, 38]. Previous studies have reported that FUBP1 is capable of promoting epithelial-mesenchymal transition of pancreatic cancer cells through the TGF- β /Smad pathway [39]. Nevertheless, the precise mechanisms of FUBP1 in pancreatic cancer remain elusive. Additionally, evidence suggests that FUBP1 can bind to non-coding RNAs and play a crucial role in tumor development. For example, FUBP1 can be recruited to *c-MYC* FUSE through lncRNA binding, resulting in the activation of *c-MYC* transcription and facilitating the proliferation, survival, invasion, and metastasis of lung cancer cells [23]. Additionally, FUBP1 can be competitively bound by circACTN4, resulting in reduced FIR-binding and subsequently triggering the activation of *c-MYC* transcription, which leads to the progression of breast cancer [24]. In this study, we revealed that tiRNA-Val-CAC-2 interacts specifically with the KH3-KH4 domains of FUBP1, leading to increased stabilization of the FUBP1 protein and its subsequent enrichment in *c-MYC* transcriptional regulation. Thus, in turn, it contributed to the transcriptional activation of *c-MYC*. It's worth mentioning that our findings indicated that tiRNA-Val-CAC-2 has the potential capacity to inhibit the ubiquitination of FUBP1 protein. As such, it is hypothesized that tiRNA-Val-CAC-2 disrupts the interaction between FUBP1 and related ubiquitin ligases in pancreatic cancer. Despite this, the specific E3 ubiquitin ligases that target FUBP1 remain elusive and require further investigation for future studies.

MATERIALS AND METHODS

Experimental procedures are provided in the Supplementary Materials.

DATA AVAILABILITY

All data and materials were available from the corresponding authors on reasonable request. The tsRNA sequencing data have been uploaded in GEO DataSets (GSE251943).

REFERENCES

- Sung H, Ferlay J, Siegel RL, Laversanne M, Soerjomataram I, Jemal A, et al. Global Cancer Statistics 2020: GLOBOCAN estimates of incidence and mortality worldwide for 36 cancers in 185 countries. *CA Cancer J Clin.* 2021;71:209–49.
- Rahib L, Smith BD, Aizenberg R, Rosenzweig AB, Fleshman JM, Matrisian LM. Projecting cancer incidence and deaths to 2030: the unexpected burden of thyroid, liver, and pancreas cancers in the United States. *Cancer Res.* 2014;74:2913–21.
- Siegel RL, Miller KD, Jemal A. Cancer statistics, 2020. *CA Cancer J Clin.* 2020;70:7–30.
- Cech TR, Steitz JA. The noncoding RNA revolution—trashing old rules to forge new ones. *Cell.* 2014;157:77–94.
- Della Bella E, Koch J, Baerenfaller K. Translation and emerging functions of non-coding RNAs in inflammation and immunity. *Allergy.* 2022;77:2025–37.
- Yu AM, Jian C, Yu AH, Tu MJ. RNA therapy: are we using the right molecules? *Pharmacol Ther.* 2019;196:91–104.
- Balatti V, Nigita G, Veneziano D, Drusco A, Stein GS, Messier TL, et al. tsRNA signatures in cancer. *Proc Natl Acad Sci USA.* 2017;114:8071–6.
- Wen JT, Huang ZH, Li QH, Chen X, Qin HL, Zhao Y. Research progress on the tsRNA classification, function, and application in gynecological malignant tumors. *Cell Death Discov.* 2021;7:388.
- Shi J, Zhang Y, Zhou T, Chen Q. tsRNAs: the Swiss army knife for translational regulation. *Trends Biochem Sci.* 2019;44:185–9.
- Kumar P, Kuscus C, Dutta A. Biogenesis and function of transfer RNA-related fragments (tRFs). *Trends Biochem Sci.* 2016;41:679–89.
- Schimmel P. The emerging complexity of the tRNA world: mammalian tRNAs beyond protein synthesis. *Nat Rev Mol Cell Biol.* 2018;19:45–58.
- Guzzi N, Ciesla M, Ngoc PCT, Lang S, Arora S, Dimitriou M, et al. Pseudouridylation of tRNA-Derived fragments steers translational control in stem cells. *Cell.* 2018;173:1204–16.e1226.
- Kim HK, Fuchs G, Wang S, Wei W, Zhang Y, Park H, et al. A transfer-RNA-derived small RNA regulates ribosome biogenesis. *Nature.* 2017;552:57–62.
- Schorn AJ, Gutbrod MJ, LeBlanc C, Martienssen R. LTR-Retrotransposon Control by tRNA-Derived Small RNAs. *Cell.* 2017;170:61–71.e11.
- Mo D, Jiang P, Yang Y, Mao X, Tan X, Tang X, et al. A tRNA fragment, 5'-tiRNA(Val), suppresses the Wnt/beta-catenin signaling pathway by targeting FZD3 in breast cancer. *Cancer Lett.* 2019;457:60–73.
- Han L, Lai H, Yang Y, Hu J, Li Z, Ma B, et al. A 5'-tRNA halve, tiRNA-Gly promotes cell proliferation and migration via binding to RBM17 and inducing alternative splicing in papillary thyroid cancer. *J Exp Clin Cancer Res.* 2021;40:222.
- Tao EW, Wang HL, Cheng WY, Liu QQ, Chen YX, Gao QY. A specific tRNA half, 5'tiRNA-His-GTG, responds to hypoxia via the HIF1alpha/ANG axis and promotes colorectal cancer progression by regulating LAT52. *J Exp Clin Cancer Res.* 2021;40:67.
- Jin F, Yang L, Wang W, Yuan N, Zhan S, Yang P, et al. A novel class of tsRNA signatures as biomarkers for diagnosis and prognosis of pancreatic cancer. *Mol cancer.* 2021;20:95.
- Xu D, Qiao D, Lei Y, Zhang C, Bu Y, Zhang Y. Transfer RNA-derived small RNAs (tsRNAs): Versatile regulators in cancer. *Cancer Lett.* 2022;546:215842.
- Tao EW, Cheng WY, Li WL, Yu J, Gao QY. tiRNAs: a novel class of small noncoding RNAs that helps cells respond to stressors and plays roles in cancer progression. *J Cell Physiol.* 2020;235:683–90.
- Honda S, Loher P, Shigematsu M, Palazzo JP, Suzuki R, Imoto I, et al. Sex hormone-dependent tRNA halves enhance cell proliferation in breast and prostate cancers. *Proc Natl Acad Sci USA.* 2015;112:E3816–3825.
- Nientiedt M, Deng M, Schmidt D, Perner S, Muller SC, Ellinger J. Identification of aberrant tRNA-halves expression patterns in clear cell renal cell carcinoma. *Sci Rep.* 2016;6:37158.
- Qian X, Yang J, Qiu Q, Li X, Jiang C, Li J, et al. LCAT3, a novel m6A-regulated long non-coding RNA, plays an oncogenic role in lung cancer via binding with FUBP1 to activate *c-MYC*. *J Hematol Oncol.* 2021;14:112.
- Wang X, Xing L, Yang R, Chen H, Wang M, Jiang R, et al. The circACTN4 interacts with FUBP1 to promote tumorigenesis and progression of breast cancer by regulating the expression of proto-oncogene MYC. *Mol cancer.* 2021;20:91.
- Li Y, Luo J, Zhou H, Liao JY, Ma LM, Chen YQ, et al. Stress-induced tRNA-derived RNAs: a novel class of small RNAs in the primitive eukaryote *Giardia lamblia*. *Nucleic Acids Res.* 2008;36:6048–55.
- Xiong Q, Zhang Y, Li J, Zhu Q. Small non-coding RNAs in human cancer. *Genes.* 2022;13:2072.

27. Cole C, Sobala A, Lu C, Thatcher SR, Bowman A, Brown JW, et al. Filtering of deep sequencing data reveals the existence of abundant Dicer-dependent small RNAs derived from tRNAs. *RNA*. 2009;15:2147–60.
28. Wu Y, Yang X, Jiang G, Zhang H, Ge L, Chen F, et al. 5'-tRF-GlyGCC: a tRNA-derived small RNA as a novel biomarker for colorectal cancer diagnosis. *Genome Med*. 2021;13:20.
29. Panoutsopoulou K, Dreyer T, Dorn J, Obermayr E, Mahner S, Gorp TV, et al. tRNA(GlyGCC)-derived internal fragment (i-tRF-GlyGCC) in ovarian cancer treatment outcome and progression. *Cancers*. 2021;14:24.
30. Li X, Zhang Y, Li Y, Gu X, Ju S. A comprehensive evaluation of serum tRF-29-R9J8909NF5JP as a novel diagnostic and prognostic biomarker for gastric cancer. *Mol Carcinog*. 2023;62:1504–17.
31. Baker LA, Holliday H, Swarbrick A. ID4 controls luminal lineage commitment in normal mammary epithelium and inhibits BRCA1 function in basal-like breast cancer. *Endocr Relat Cancer*. 2016;23:R381–92.
32. Zhu L, Li J, Gong Y, Wu Q, Tan S, Sun D, et al. Exosomal tRNA-derived small RNA as a promising biomarker for cancer diagnosis. *Mol Cancer*. 2019;18:74.
33. Chen Q, Zhang X, Shi J, Yan M, Zhou T. Origins and evolving functionalities of tRNA-derived small RNAs. *Trends Biochem Sci*. 2021;46:790–804.
34. Yu M, Lu B, Zhang J, Ding J, Liu P, Lu Y. tRNA-derived RNA fragments in cancer: current status and future perspectives. *J Hematol Oncol*. 2020;13:121.
35. Cui H, Li H, Wu H, Du F, Xie X, Zeng S, et al. A novel 3'tRNA-derived fragment tRF-Val promotes proliferation and inhibits apoptosis by targeting EEF1A1 in gastric cancer. *Cell Death Dis*. 2022;13:471.
36. Yang W, Gao K, Qian Y, Huang Y, Xiang Q, Chen C, et al. A novel tRNA-derived fragment AS-tDR-007333 promotes the malignancy of NSCLC via the HSPB1/MED29 and ELK4/MED29 axes. *J Hematol Oncol*. 2022;15:53.
37. Braddock DT, Louis JM, Baber JL, Levens D, Clore GM. Structure and dynamics of KH domains from FBP bound to single-stranded DNA. *Nature*. 2002;415:1051–6.
38. Debaize L, Troadec MB. The master regulator FUBP1: its emerging role in normal cell function and malignant development. *Cell Mol Life Sci*. 2019;76:259–81.
39. Zhang Y, Chen J, Zhou N, Lu Y, Lu J, Xing X, et al. FUBP1 mediates the growth and metastasis through TGFβ/Smad signaling in pancreatic adenocarcinoma. *Int J Mol Med*. 2021;47:66.

ACKNOWLEDGEMENTS

We sincerely thank our colleagues (Zhou Zhao, Lingli Wang, Lei Qiu, Xiaobing Mao, Yang Meng, Sicheng Liu, Yang Zhang, Qian Jing, Qin Chen, Qing Huang, etc.) for the constructive suggestions for this study. We also thank Animal Experimental Center, West China Hospital for providing the platform for animal experiments. This research was funded by the Natural Science Foundation of Sichuan (2023NSFSC0719) and 1.3.5 Project for Disciplines of Excellence, West China Hospital, Sichuan University (ZYJC21042, ZYGD23017), and National Natural Science Foundation of China (82203447).

AUTHOR CONTRIBUTIONS

Conceptualization: QLX and QZ. Original draft writing and editing: QLX, YGZ and JHH. Figure creating: QLX, YGZ, YFX, YY, ZWZ, YZ, SZ, LZ, XWW, XJY, ZZ (Zhu Zeng), JLL and

ZZ (Ying Zheng). Resources, supervision, funding acquisition and revision: YGZ, JHH and QZ.

COMPETING INTERESTS

The authors declare no competing interests.

ETHICAL APPROVAL

All experiments using specimens were approved by the ethics committee and performed strictly abiding by relevant regulations of the Declaration of Helsinki under the prerequisite of obtaining written informed consent, and approved by the Ethics Committee of West China Hospital, Sichuan University (approval number: 20211189). For animal study: the study was approved by the Experimental Animal Welfare Ethics Committee, West China Hospital of Sichuan University (approval number: 20220505002).

ADDITIONAL INFORMATION

Supplementary information The online version contains supplementary material available at <https://doi.org/10.1038/s41388-024-02991-9>.

Correspondence and requests for materials should be addressed to Junhong Han or Qing Zhu.

Reprints and permission information is available at <http://www.nature.com/reprints>

Publisher's note Springer Nature remains neutral with regard to jurisdictional claims in published maps and institutional affiliations.



Open Access This article is licensed under a Creative Commons Attribution 4.0 International License, which permits use, sharing, adaptation, distribution and reproduction in any medium or format, as long as you give appropriate credit to the original author(s) and the source, provide a link to the Creative Commons licence, and indicate if changes were made. The images or other third party material in this article are included in the article's Creative Commons licence, unless indicated otherwise in a credit line to the material. If material is not included in the article's Creative Commons licence and your intended use is not permitted by statutory regulation or exceeds the permitted use, you will need to obtain permission directly from the copyright holder. To view a copy of this licence, visit <http://creativecommons.org/licenses/by/4.0/>.

© The Author(s) 2024